

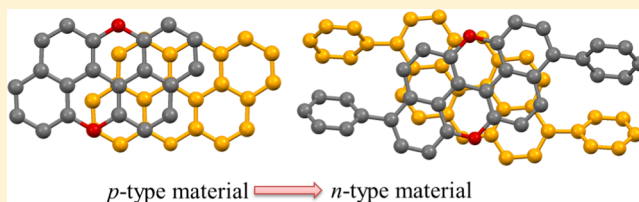
Electronic and Charge Transport Properties of *peri*-Xanthenoxanthene: The Effects of Heteroatoms and Phenyl Substitutions

Lijuan Wang, Guihua Duan, Yanan Ji, and Houyu Zhang*

State Key Laboratory of Supramolecular Structure and Materials, Jilin University, Changchun 130012, P. R. China

S Supporting Information

ABSTRACT: The electronic and charge transport properties of *peri*-xanthenoxanthene (PXX) and its phenyl-substituted derivative (Ph-PXX) are explored via quantum chemical calculations. To gain a better understanding of the physical properties of PXX, a comparative study is performed for its analogue, that is, anthanthrene. By employing Marcus electron transfer theory coupled with an incoherent charge hopping and diffusion model, we estimate the charge mobilities of PXX and Ph-PXX. Our calculated results indicate that the introduction of a heteroatom (oxygen) at the reactive sites of anthanthrene can stabilize the extended π -system and improve the efficient charge injection in electronic devices. The phenyl substitution of PXX makes a remarkable change of charge transport characteristics from a *p*-type semiconductor to an *n*-type semiconductor, which shed light on molecular design for an *n*-type semiconductor through simple chemical structural modification.



INTRODUCTION

The advances in the development of high performance organic semiconductors (OSCs) for field-effect transistors (FETs) have been boosted rapidly in recent years since the first report in 1986.¹ Though significant progress has been made by promoting the mobility of OSCs from $\sim 10^{-5} \text{ cm}^2 \text{ V}^{-1} \text{ s}^{-1}$ for polythiophene¹ to more than $10 \text{ cm}^2 \text{ V}^{-1} \text{ s}^{-1}$ for organic thin film² and single crystal,³ there remain some key challenges such as the need to improve mobility, achieve high air-stability, as well as seek for more *n*-type and ambipolar semiconductors.⁴

In order to gain higher mobility, a promising strategy is utilizing extended π -systems to enhance the overlap of molecular orbitals between neighboring molecules. Examples of large π -conjugated systems in FETs are acenes, thiophenes, phthalocyanine, perylene, naphthalene, and their diversity of derivatives.^{5,6} In the case of acenes, large members of the acene family appear to be so reactive that they can only be probed by theory. The synthetic accessibility of oligoacenes is limited to hexacene, and a thorough understanding of electronic properties hovers at pentacene. Unfortunately, pentacene is easily oxidized when exposed to oxygen. The hydrogens at the 6 and 13 positions at the central benzene ring of pentacene are replaced by oxygens, which will destroy the conjugation of the central π -conjugated systems. Once a molecule is oxidized, it will no longer participate in the charge-carrier transport of the transistor, leading to the mobility decreased monotonically and irreversibly. So air-stability of OSCs is another important issue that researchers have to pay more attention to. OSCs with a larger ionization potential (IP) and thus better oxidation resistance would be expected. On the other hand, the larger IP or deep highest occupied molecular orbital (HOMO) will lead to a higher energy barrier for charge (hole) injection. So the

balance between larger IP and charge injection barrier is of great importance for high performance OFETs. Besides the pursuit of high mobility and air-stability of OSCs, the search for *n*-type OSCs with high performance and high stability is still a challenging issue.^{7,8} The chemical modification with strong electronegative substituents is an effective approach for converting *p*-type materials to *n*-type.^{4,9}

Recently, a stable transistor by using Ph-PXX as active semiconductor layer with efficient carrier injection was reported.¹⁰ The large π -conjugated system in PXX is expected to enhance the overlap of molecular orbitals. Compared with anthanthrene, the introduction of heteroatoms (oxygen) and phenyl groups into the π -system make the reactive sites inactive, which can improve the environmental stability of Ph-PXX. The preliminary study of the IPs of PXX and Ph-PXX have been carried out by DFT calculations to demonstrate the matching of the HOMO level with the workfunction of metal electrode, which ensures efficient carrier injection.¹⁰ What is still lacking is a deep understanding of the relationship between the modified structures and the resulting electronic properties in a microscopic level. The influence of heteroatoms and phenyl group on the stability and charge transport properties should be elucidated in detail. The phenyl substitutions on PXX will affect the molecular arrangement and thus might alter the charge transport properties. Moreover, from the molecular design point of view, deep understanding of the electronic and charge transport properties of OSCs will shed light on the design strategy for both materials themselves and device

Received: June 27, 2012

Revised: October 4, 2012

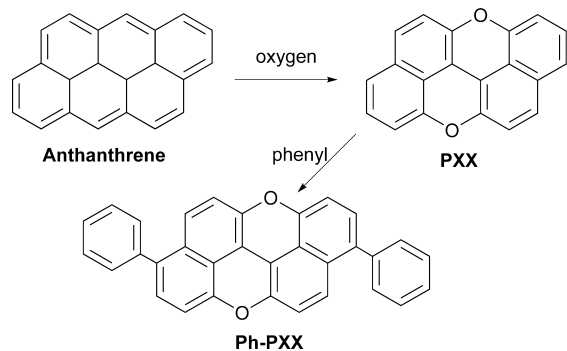
Published: October 6, 2012

architectures. In view of the importance of substitution of heteroatoms and phenyl group, herein we will theoretically investigate the electronic and charge transport properties of PXX and Ph-PXX.

Theoretical calculation is becoming a powerful tool to study the charge transport properties of OSCs and predict the drift mobilities.^{11–21} At a high-temperature regime and in the presence of structural disorders, charge carriers are localized over a single molecule, which make the bandlike mechanism fail in describing the transport behavior in many OSCs. Thus, a thermally activated hopping and diffusion model is employed to simulate the charge carrier motion. Whether charge transport occurs by a hopping or bandlike mechanism, the mobility of OSCs is determined by molecular arrangement in the solid state. The crystal structure of organic material which has definite structural information provides a model for fundamentally understanding the correlation between packing motifs and the resulting charge transport phenomena. In this regard, a deep understanding of electronic structure of OSCs will be definitely useful in correlating transport properties with chemical structures and molecular packing in OSCs.

In present work, we use quantum chemical calculation to make comparative studies of the electronic properties of PXX, Ph-PXX, and their analogue, anthanthrene (as illustrated in Scheme 1). We will focus on the effect of heteroatom and

Scheme 1. Chemical Structures of Anthanthrene, *peri*-Xanthenoxanthene (PXX), and Phenyl-Substituted *peri*-Xanthenoxanthene (Ph-PXX)



phenyl substitution on the electronic structure. By means of density functional theory (DFT) calculations, we aim to establish structure–property relationships of PXX materials and shed light on the fundamental research and design of high charge mobility materials.

THEORETICAL AND COMPUTATIONAL METHOD

The molecular geometries of neutral and charged states are optimized at the DFT level using B3LYP hybrid functional^{22,23} and 6-31G** basis set, as implemented in the Gaussian 09 package.²⁴ Harmonic vibrational frequencies are calculated at the same level of theory on the basis of resulting optimized geometries. The molecular ionization potential (IP) and electron affinity (EA) are calculated at the basis of 6-31++G** in comparison with 6-31G**. The total density of state (DOS) and projected density of state (PDOS) for oxygen atom and phenyl group are obtained with GaussSum 2.25 program.²⁵

To study the charge transport properties of PXX and Ph-PXX at room temperature, here we adopt the hopping transport model to describe the carrier motion process.

According to the Einstein relation, the drift mobility, μ , is related to the diffusion coefficient D as

$$\mu = \frac{e}{k_B T} D; \quad D = \frac{1}{2n} \sum_i d_i^2 k_i P_i \quad (1)$$

where e is the electronic charge, k_B is the Boltzmann constant, T is the room temperature (298 K). Considering the charge motion as a random walk in three dimensions ($n = 3$), the diffusion coefficient is the summation over all the possible hops between neighboring molecules. k_i and P_i are hopping rate and the probability ($P_i = k_i / \sum k_i$) for charge transfer to i th neighbor. d_i is the intermolecular center-to-center distance.

For each charge hopping event from a charged molecule to a neighboring neutral molecule, the self-exchange charge transfer rate can be expressed by Marcus theory²⁶ in terms of reorganization energy and electronic coupling V_{ab} between neighboring molecules a and b :²⁷

$$k = \frac{2\pi V_{ab}^2}{h} \left(\frac{\pi}{\lambda k_B T} \right)^{1/2} \exp\left(-\frac{\lambda}{4k_B T}\right) \quad (2)$$

The charge hopping rate benefits from larger V_{ab} and smaller λ .

The reorganization energy usually contains two parts: the internal reorganization energy (which is induced by intramolecular vibrations) and the external reorganization energy (which is caused by polarization of the surrounding medium). For organic solids and weak polar media, the contribution to the reorganization energy from electronic polarization of surrounding molecules is quite small and is on the order of a few tenths of an electronvolt,^{28–31} so the external reorganization energy is neglected. Neglecting the external reorganization energy leads to the enhanced results for molecular conductors. While the intermolecular tunneling, especially the contribution from the higher frequency vibrational normal modes, is also critical to the charge transfer rate. So in some sense, neglect of tunneling will compensate for the neglect of the external reorganization energy.²¹ Herein, only the intramolecular reorganization energy is calculated. The internal reorganization energy is calculated directly from the relevant points on the adiabatic potential energy surfaces (PES) using the standard procedure detailed in the literature.^{32,33} For comparison, the reorganization energy is also evaluated on the basis of normal-mode analysis (NMA) method with the DUSHIN code³⁴ using the results of the frequency calculations. In a displaced harmonic oscillator model, total reorganization energy is obtained as summation of all the vibrational modes:^{32,35}

$$\lambda = \sum_i \lambda_i = \sum_i \frac{1}{2} \omega_i^2 \Delta Q_i^2 \quad (3)$$

Here, ΔQ_i is the displacement between equilibrium geometries of the neutral and charged molecules for normal mode i , and ω_i is the vibrational frequency.

The electronic couplings V_{ab} , which measure the degree of molecular orbital overlapping between charge donor and acceptor, are calculated through a direct approach using Fock operator acting on the two interacting frontier orbitals of neighboring molecules^{36,37}

$$V_{ab} = \langle \Psi_i^{0,a} | F | \Psi_i^{0,b} \rangle \quad (4)$$

where $\Psi_i^{0,a}$ and $\Psi_i^{0,b}$ represent the molecular frontier orbitals of isolated molecules a and b , and where i denotes the highest occupied molecular orbitals (HOMO) for hole transfer and

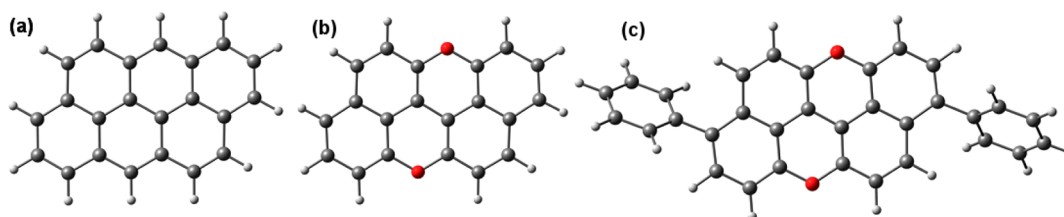


Figure 1. Optimized structures of anthanthrene (a), PXX (b), and Ph-PXX (c).

lowest unoccupied molecular orbitals (LUMO) for electron transfer. F^0 is the Fock operator for the dimer in a specific pathway, and the superscript zero indicates that the molecular orbitals appearing in the operator are unperturbed. The Fock matrix can be evaluated by $F = SC\epsilon C^{-1}$, with S is the intermolecular overlap matrix, and C and ϵ are the molecular orbital coefficients and eigenvalues, respectively. Using the standard self-consistent-field procedure, the molecular orbitals and density matrix of the two individual molecules are calculated separately. These are used to evaluate the Kohn–Sham–Fock matrix of the dimer structure. All the electronic coupling calculations are carried out using B3LYP functional with 6-31G(d) basis set due to the computational costs for all the possible pathways in all crystal structures. To estimate the intermolecular interaction energy, a dispersion corrected B97-D functional^{38,39} with large basis set 6-311++G** is employed for the single point energy calculations. The interaction energy is obtained as the energy difference between the energy of dimer and the sum of total energies of two interacting monomers.

To evaluate the electronic couplings between the dimer molecules, the crystal structures of PXX and Ph-PXX are used to define the dimer configurations. The crystal structure provides three-dimensional molecular alignments, which define the three-dimensional charge diffusion model in specific routes. The definite structural information in the crystal provides a model to understand the correlations between the molecular packing motifs and electronic couplings between molecules, as well as the mobility in the solid state.

RESULTS AND DISCUSSION

Molecular Geometries and Reorganization Energies.

The optimized structures in the neutral state of anthanthrene, PXX, and Ph-PXX are shown in Figure 1. PXX exhibits a planar and rigid skeleton, which is the same as its analogue, anthanthrene. The phenyl rings in Ph-PXX have torsional angles of 54.4° relative to central fused π system, which is in good agreement with experimental crystal structure (53.8°).¹⁰ When a molecule gains or loses charges, it will relax its molecular geometry for a new charge distribution. The above-mentioned torsional angles in Ph-PXX are 50.9° and 45.6° for the cationic state and anionic state, respectively. The bond-length changes upon oxidation (losing electron from the neutral to the cation state) and reduction (gaining electron from the neutral to the anion state) of anthanthrene, PXX, and Ph-PXX are shown in Figure 2. Because of the extended π -system, the bond-length changes upon oxidation and reduction are found to occur over the entire molecule, especially in the fused rings. The geometrical changes in PXX and Ph-PXX are more pronounced than those in anthanthrene, which can be regarded as the effect of introduction of oxygen atom in the system. The bond-length changes for bonds 4, 5, 12, and 13 are quite different from those in anthanthrene. The bond-length changes upon reduction for three compounds are significantly

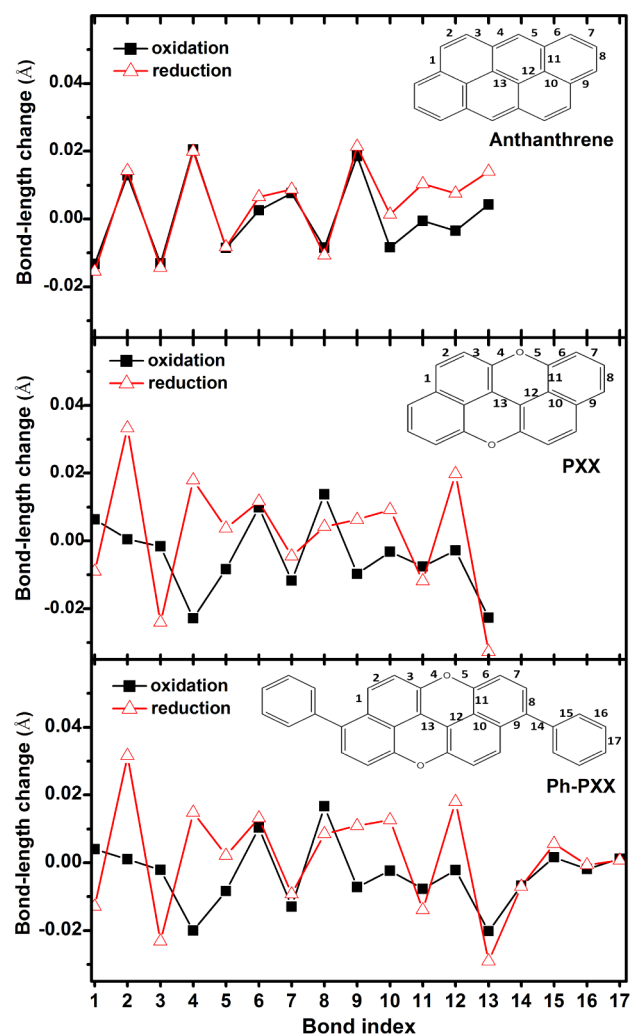


Figure 2. Bond-length changes (in Å) upon oxidation and reduction in anthanthrene, PXX, and Ph-PXX. The bond indices are labeled on the molecular structures.

larger than those upon oxidation; this indicates that the reorganization energies for electron are substantially larger than those for hole of the investigated molecules.

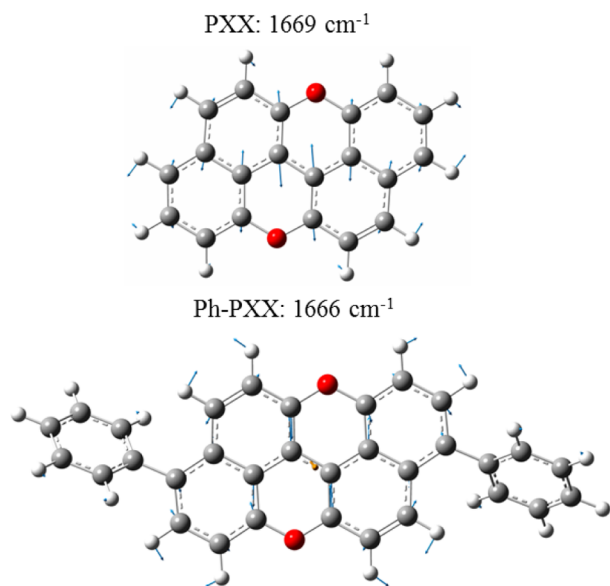
Internal reorganization energies for hole and electron calculated by both adiabatic PES method and NMA method are listed in Table 1. Results from two methods show reasonable agreement; this indicates that the displaced harmonic oscillator model is suitable for describing the charge reorganizing process. The reorganization energies for electron are higher than those for hole of three compounds. According to eq 2, the charge transport rate favors small reorganization energy. From the reorganization energy point of view, all three compounds are in favor of transporting hole rather than

Table 1. Calculated Reorganization Energies for Hole and Electron

compd	reorganization energy (eV)			
	hole		electron	
	PES	NM	PES	NM
PXX	0.156	0.156	0.301	0.303
Ph-PXX	0.154	0.154	0.336	0.338
anthanthrene	0.117	0.118	0.155	0.156

electron. The oxygen atoms in the π system increase the reorganization energies for both hole and electron. The reorganization energy for electron of PXX is 0.301 eV, which is nearly 2 times of that for anthanthrene (0.155 eV). Compared with PXX, the substitution of phenyl groups does not increase the reorganization energy for hole, but slightly increases the reorganization energy for electron. The higher reorganization energy is supported by a larger geometrical relaxation with respect to the neutral geometry, as can be seen in Figure 2.

To further analyze the origin of the reorganization energy, the reorganization energies for hole and electron of PXX and Ph-PXX are decomposed into contributions from individual normal modes,³⁴ as listed in the Tables S1 and S2 in the Supporting Information. The vibrational modes yielding the largest contribution to the reorganization energies for hole are 1669 and 1666 cm^{-1} for PXX and Ph-PXX, respectively. These two modes belong to the stretching motion of C–C bonds in the conjugated π -system, as depicted in Figure 3. While the

**Figure 3.** Normal modes that contributes the most of reorganization energy for holes of PXX and Ph-PXX.

main contributions to the reorganization energy for electron for PXX and Ph-PXX are in the range 1350–1650 cm^{-1} . The modes with reorganization energy larger than 120 cm^{-1} are at 1404, 1562, 1600, and 1606 cm^{-1} for PXX, and at 1397, 1516, 1538, and 1588 cm^{-1} for Ph-PXX, as depicted in Figure 4. These high frequency vibrational modes mentioned above not only contribute most of the internal reorganization energy, but also might be responsible for the intermolecular tunnelings,

which play an important role in charge transfer rate and are usually neglected in the charge hopping mechanism.

Molecular Ionization Potential and Electron Affinity. It is well-known that efficient injection of holes and electrons is important for the rational design of optimized electronic devices. The molecular ionization potential (IP) and electronic affinity (EA) are very key parameters pertaining to charge injection, which can provide useful information regarding the organic device performance and its ambient stability. IPs and EAs are used to estimate the energy barrier for injection of hole and electron into molecule. The calculated IPs and EAs of compounds, both vertical (at the geometry of the neutral molecule) and adiabatic (optimized structure for both the neutral and charged molecules), are presented in Table 2. In comparison with the calculated values from basis sets of 6-31++G** and 6-31G** (values in parentheses), we can see that these results are very dependent on the diffuse function of basis set, especially for the EAs.

DFT-B3LYP calculations predict a decrease in the adiabatic ionization potential upon oxygen and phenyl-substitution. Compared with anthanthrene, PXX and Ph-PXX have decreases of 0.11 and 0.34 eV, respectively. The IPs of PXX and Ph-PXX are comparable to that of typical compound pentacene. Though the decreased IPs make the compounds less stable and readily oxidized, the substitutions on the most active site of anthanthrene make these compounds more antioxidative, which make it possible in practical applications. For the commonly used Au electrodes, Ph-PXX is expected to have smaller injection energy for hole than PXX and anthanthrene.

The EA values of PXX and Ph-PXX are -0.50 and -0.67 eV, respectively (see Table 2 for the adiabatic value of EAs). The introduction of oxygen and phenyl group makes the EAs less exothermic. (The negative values of EAs indicate exothermicity for the reduction of molecules; e.g., Ph-PXX is 0.4 eV less exothermic than that of anthanthrene.) In the devices, the smaller EA value means the larger injection energy for electron, referring to commonly used metallic electrodes (3 eV). The more exothermic value means more stability for the anionic species of compounds toward reaction with water and oxygen. From these EA values, we can see that Ph-PXX is better than PXX for transporting electrons from both lowering the energy barrier for electron injection and stability of their anionic species. For the practical applications in a device, a suitable electrode is required for electron mobility measurement for Ph-PXX. The differences between vertical and adiabatic values reflect the extent of the structural relaxation upon charge injection.

Molecular Orbitals and Density of States. Frontier orbitals, especially HOMOs and LUMOs, are closely related to gain and loss of electrons. The introduction of oxygen and phenyl group will definitely affect the frontier orbitals of the anthanthrene. To further investigate the composition of orbitals near the HOMO–LUMO gap, we calculated the PDOS for oxygen atom and phenyl group and total DOS for three compounds, as shown in Figure 5. The HOMO and LUMO of three compounds are inserted in Figure 5. The majority of the molecular orbital density in the HOMO and LUMO is mainly from the delocalized π -orbital of central rings. The contributions from oxygen atom and ending phenyl group to the molecular orbitals are shown in the plot of projected density of state as displayed in Figure 5. There is a notable contribution to HOMO and LUMO from oxygen atoms in PXX and Ph-PXX compounds. Compared with anthanthrene, the oxygen atoms in

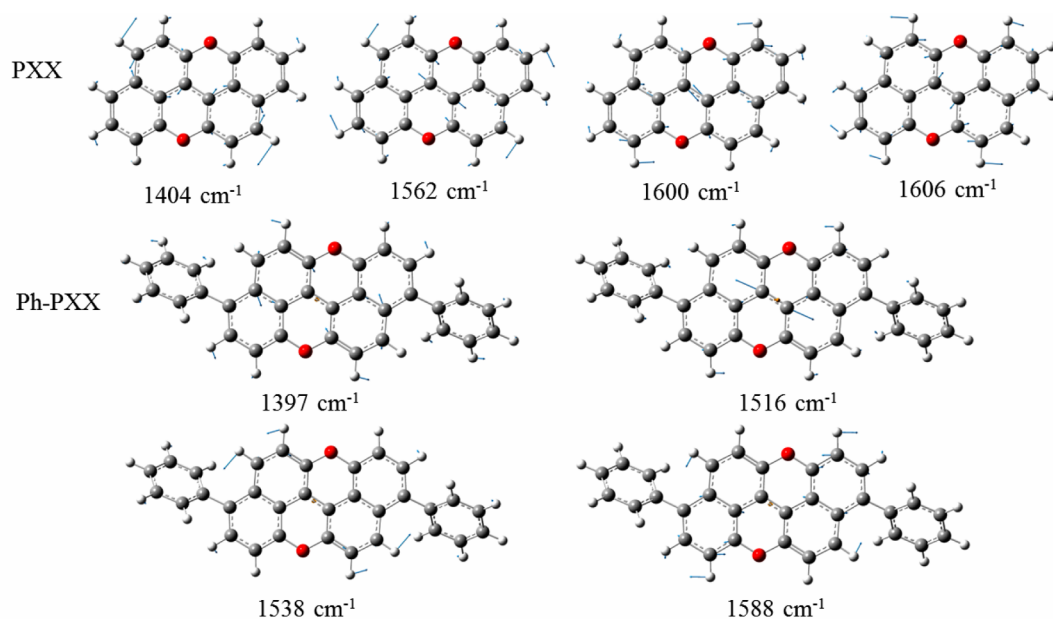


Figure 4. Normal modes that contributes the most of reorganization energy for electrons of PXX and Ph-PXX.

Table 2. Ionization Potential (IP) and Electron Affinity (EA) of PXX, Ph-PXX, and Anthanthrene,^a in Comparison with Those Values for Typical Compound Pentacene

compd	IP (eV)		EA (eV)	
	vertical	adiabatic	vertical	adiabatic
PXX	6.43 (6.19)	6.36 (6.12)	-0.35 (-0.058)	-0.50 (-0.09)
Ph-PXX	6.21 (5.96)	6.13 (5.88)	-0.52 (-0.14)	-0.67 (-0.31)
anthanthrene	6.53 (6.31)	6.47 (6.25)	-0.99 (-0.63)	-1.07 (-0.70)
pentacene ^b	6.17 (5.95)	6.13 (5.90)	-1.42 (-1.07)	-1.49 (-1.14)

^aAll calculations are carried out using the basis sets of 6-31++G** and 6-31G** (values in parentheses). ^bFrom ref 16.

the PXX and Ph-PXX break the conjugation of π orbitals, which makes the HOMO–LUMO energy gap enlarge. The HOMO–LUMO gap is 3.28 (3.21) eV for PXX (Ph-PXX), whereas the HOMO–LUMO gap for anthanthrene is 2.88 eV. The phenyl groups in Ph-PXX can extend the delocalized the π orbitals, making the HOMO–LUMO gap a little bit narrow compared with PXX.

Focusing on the frontier orbitals in Ph-PXX, we found that the oxygen atoms are involved in the formation of HOMO and LUMO, whereas the phenyl groups contribute little to the formation of HOMO and LUMO. For the phenyl groups, they largely participate in the HOMO+3, HOMO+4, LUMO–3, and LUMO–4. From the electronic structure point of view, the oxygen atoms take part in the formation of frontier orbitals HOMOs and LUMOs, and directly involve the charge carrier transport. Because of the dihedral angle between phenyl group with the central π systems, the phenyl groups can not extend the conjugation of π system largely. The phenyl groups only partly involve the charge transport. But from the molecular structure point of view, the phenyl group will affect the molecular arrangement. The substitution of oxygen atoms and phenyl groups will affect the frontier intermolecular orbital interactions, resulting in the different electronic couplings for hole and electron.

Electronic Coupling and Mobility. To define the charge hopping pathways, we use the single crystal structures to generate a wide variety of possible intermolecular hopping

pathways. The crystal structure and charge hopping pathways scheme are displayed in Figure 6. Choose one molecule as charge donor, and then all the nearest neighbor molecules can be regarded as charge acceptor. The geometries of dimer pairs are selected from crystal structure, and the intermolecular mass-center distances are shown in Table 3. The multimolecules configurations shown in Figure 6 are defined by lattice plane, in which the electronic coupling V_{ab} values larger than 0.1 meV are shown. For example, in the PXX crystal, from the view along a axis, we can see that there are six molecules around the centered molecule. These 7 molecules are located in the bc plane. While from the view along b axis, only 2 molecules are selected. Thus, we selected 12 pathways from all possible 26 hopping pathways from the centered molecule in PXX crystal. For Ph-PXX crystal, we selected 14 pathways as shown in Figure 6b. We calculated all the electronic coupling between the dimer molecules for each compound through the direct evaluation methods of eq 4, which are reported in Table 3. In PXX crystal, besides the moderate electronic couplings through herringbone configurations (3, 4, 5, and 6) and side-by-side configurations (11 and 12), the most prominent pathways for charge transfer are routes 1 and 2, which are through a displaced π -stacking configurations, as displayed in Figure 7a. The vertical and displaced distances between the stacked PXX molecules are about 3.4 and 3.6 Å, respectively. The electronic coupling for hole and electron are 45.6 and 23.9 meV, respectively. The pictorial orbital interactions between

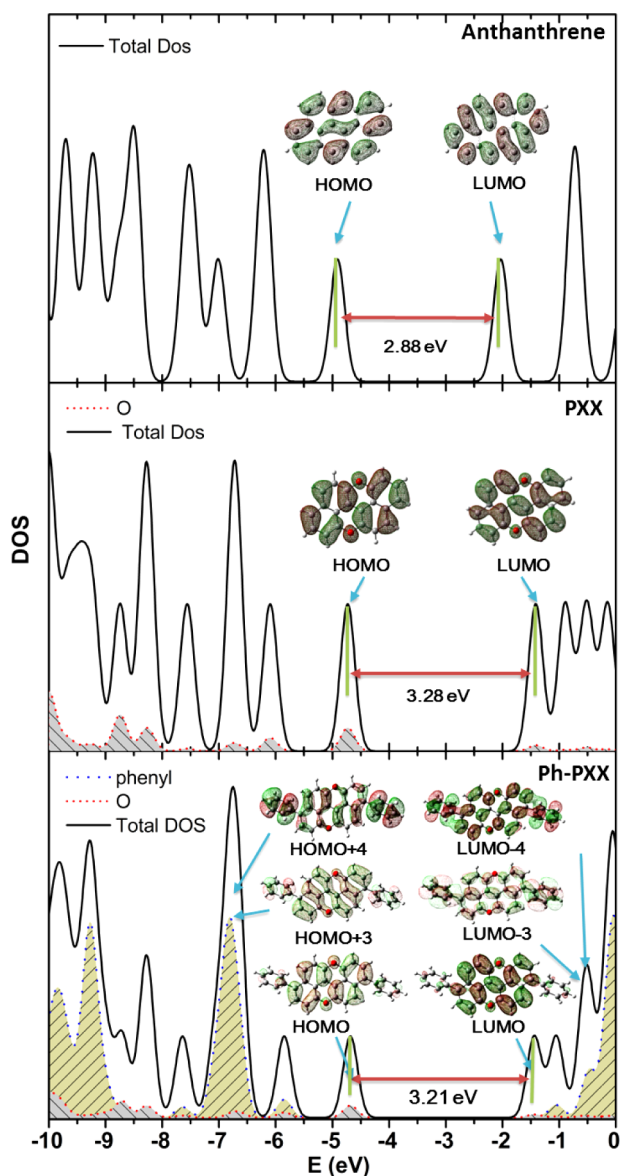


Figure 5. Total DOS and PDOS for oxygen atom and phenyl group in the energy window of -10 and 0 eV for anthanthrene, PXX, and Ph-PXX.

HOMOs and LUMOs are shown in Figure 7. We can see that the overlapping of interacting HOMOs and LUMOs in the displaced configurations are very obvious. While in Ph-PXX crystal, the determinant routes (1 and 2) for charge transfer are through the π -stacking interaction. The difference from the displaced stacking in PXX is rotated stacking in Ph-PXX, as displayed in the topview picture of two stacked molecules. The strong $\text{CH}\cdots\pi$ interactions at the ending phenyl groups (edge-to-face) make the two Ph-PXX molecules on top of each other. Because of the strong repulsion interactions, the distance between the two molecules is about 3.5 Å, slightly larger than that in displaced PXX stacking configuration. The two molecules prefer maintaining in a rotated manner with the angle between the molecular long axis being about 52° . The DFT-B97D calculated the interaction energy between dimer molecules in Figure 7 as 19.6 and 33.4 kcal/mol for PXX and Ph-PXX, respectively. The function of phenyl substitution affords a strong intermolecular interaction (edge-to-face CH/π

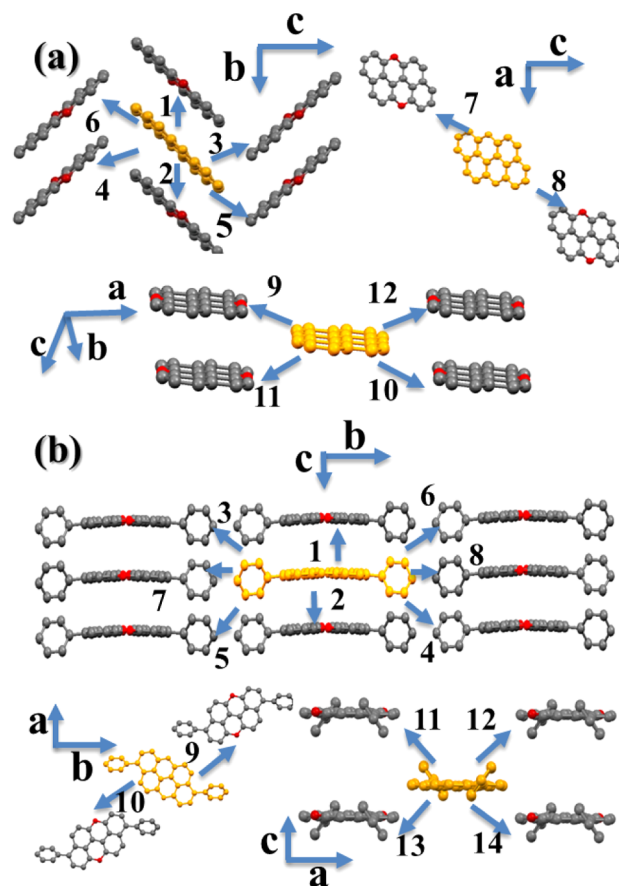


Figure 6. Charge hopping pathways for PXX (a) and Ph-PXX (b).

Table 3. Electronic Coupling V_{ab} of Hole and Electron for All Pathways for Two Compounds

pathway	distance (Å)	H_{ab}^h (meV)	H_{ab}^e (meV)
PXX			
1, 2	4.98	45.6	23.9
3, 4, 5, 6	8.46	6.2	2.3
7, 8	11.22	0.08	0.8
9, 10	8.35	0.6	0.2
11, 12	8.35	3.6	7.9
Ph-PXX			
1, 2	3.47	2.6	140.6
3, 4, 5, 6	18.83	0.3	2.1
7, 8	18.51	0.5	0.1
9, 10	12.25	0.1	0.4
11, 12	13.03	2.4	0.6
13, 14	12.43	1.8	0.1

interaction) to hold the molecular packing configuration. Surprisingly, the electronic coupling for electron in Ph-PXX is 140 meV, which is larger than that for hole (2.6 meV). From the dimer configurations in PXX and Ph-PXX, we know that phenyl group substitution changes the molecular arrangements, leading to the difference of electronic coupling strength. In Ph-PXX, the small electronic coupling for HOMOs can be attributed to the cancellation between the bonding and antibonding overlaps.⁴⁰ Such simple substitutions of phenyl groups alter the electronic coupling feature from being beneficial to hole in PXX to electron in Ph-PXX.

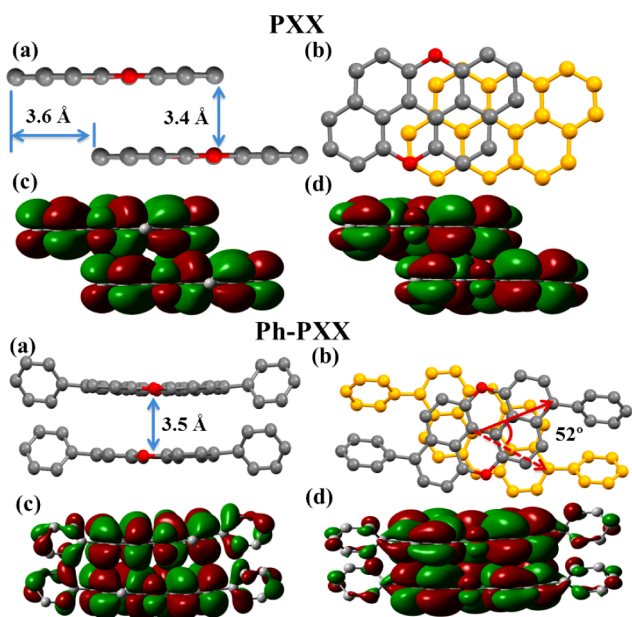


Figure 7. π - π stacking configurations in PXX and Ph-PXX: side view (a) and top view (b) for the dimer geometries, and pictorial orbital interaction for HOMOs (c) and LUMOs (d).

The theoretical predicted diffusion mobilities for PXX compounds in crystal state at room temperature for hole and electron are 0.31 and 0.01 $\text{cm}^2 \text{V}^{-1} \text{s}^{-1}$, respectively. However, for Ph-PXX crystal the predicted values for hole and electron are 0.003 and 0.17 $\text{cm}^2 \text{V}^{-1} \text{s}^{-1}$, respectively. The calculated mobilities are on the same order as their experimental values¹⁰ (e.g., for Ph-PXX, 0.4 $\text{cm}^2 \text{V}^{-1} \text{s}^{-1}$). PXX prefers transporting holes, while Ph-PXX prefers electron transport. Though such conversion needs to be verified by more experiments, it provides a possible way to design *n*-type transport materials.

Comments on Design *n*-Type FET Materials. It is well-known that a common approach to design electron transporting materials from typical hole transporting material is to functionalize *p*-type semiconductors with strong electron withdrawing substituents, such as perfluorophenyl,⁴¹ carbonyl,⁴² and cyano groups.⁹ In this work we show that the conversion from *p*-type materials (PXX) to *n*-type materials (Ph-PXX) can be realized through simple chemical modifications, e.g., phenyl substitution. The phenyl groups afford dual roles in the crystal state: (1) change the molecular packing arrangements from slipped stacking to on-top-of-each-other stacking, leading to the characteristic of transfer integral changed from being in favor of hole to electron; (2) provide strong intermolecular interaction energy to stabilize dimer configuration. To date, a great number of π -conjugated semiconducting materials have been synthesized to enrich the library of π -conjugated systems for use in organic electronics, especially for *p*-type materials. The structural versatility of an organic semiconductor allows for the incorporation of functionality by molecular design. As long as we understand the fundamental knowledge regarding structure–property relationships behind the structural design, we will realize the molecular design with desired properties (e.g., from *p*- to *n*-type) by chemical modification.

CONCLUSIONS

In conclusion, the electronic and charge transport properties of *peri*-xanthenoxanthene have been investigated by DFT calculations. The introduction of heteroatom oxygen and phenyl group at the active sites in the π -conjugated system can promote the air stability. The oxygen atoms in PXX and Ph-PXX do not affect the molecular planarity, and slightly break the conjugation. The phenyl substitution of PXX makes a remarkable change of charge transport characteristics from *p*-type semiconductor to *n*-type semiconductor, which sheds light on molecular design for *n*-type semiconductors through simple chemical modification.

ASSOCIATED CONTENT

Supporting Information

Additional tables. This material is available free of charge via the Internet at <http://pubs.acs.org/>.

AUTHOR INFORMATION

Corresponding Author

*E-mail: houyuzhang@jlu.edu.cn.

Notes

The authors declare no competing financial interest.

ACKNOWLEDGMENTS

We are grateful for the financial support from the National Nature Science Foundation of China (Grants 21173101 and 21073077), and the Major State Basic Research Development Program (2009CB623600). L.W. acknowledges the support of Graduate Innovation Fund of Jilin University (No. 20121055).

REFERENCES

- (1) Tsumura, A.; Koezuka, H.; Ando, T. *Appl. Phys. Lett.* **1986**, *49*, 1210–1212.
- (2) Li, L.; Tang, Q.; Li, H.; Yang, X.; Hu, W.; Song, Y.; Shuai, Z.; Xu, W.; Liu, Y.; Zhu, D. *Adv. Mater.* **2007**, *19*, 2613–2617.
- (3) Jurchescu, O. D.; Popinciuc, M.; van Wees, B. J.; Palstra, T. T. M. *Adv. Mater.* **2007**, *19*, 688–692.
- (4) Dong, H.; Wang, C.; Hu, W. *Chem. Commun.* **2010**, *46*, 5211–5222.
- (5) Bendikov, M.; Wudl, F.; Perepichka, D. F. *Chem. Rev.* **2004**, *104*, 4891–4946.
- (6) Wang, C.; Dong, H.; Hu, W.; Liu, Y.; Zhu, D. *Chem. Rev.* **2012**, *112*, 2208–2267.
- (7) Chang, Y.-C.; Kuo, M.-Y.; Chen, C.-P.; Lu, H.-F.; Chao, I. *J. Phys. Chem. C* **2010**, *114*, 11595–11601.
- (8) Jung, B. J.; Tremblay, N. J.; Yeh, M.-L.; Katz, H. E. *Chem. Mater.* **2011**, *23*, 568–582.
- (9) Kuo, M.-Y.; Chen, H.-Y.; Chao, I. *Chem.—Eur. J.* **2007**, *13*, 4750–4758.
- (10) Kobayashi, N.; Sasaki, M.; Nomoto, K. *Chem. Mater.* **2009**, *21*, 552–556.
- (11) Deng, W. Q.; Goddard, W. A., III. *J. Phys. Chem. B* **2004**, *108*, 8614–8621.
- (12) Yang, X. D.; Wang, L. J.; Wang, C. L.; Long, W.; Shuai, Z. *Chem. Mater.* **2008**, *20*, 3205–3211.
- (13) Wang, C. L.; Wang, F. H.; Li, Q. K.; Shuai, Z. G. *Org. Electron.* **2008**, *9*, 635–640.
- (14) Wen, S.-H.; Li, A.; Song, J.; Deng, W.-Q.; Han, K.-L.; Goddard, W. A. *J. Phys. Chem. B* **2009**, *113*, 8813–8819.
- (15) Wen, S.-H.; Deng, W.-Q.; Han, K.-L. *Phys. Chem. Chem. Phys.* **2010**, *12*, 9267–9275.
- (16) Delgado, M. C. R.; Pigg, K. R.; da Silva Filho, D. A.; Gruhn, N. E.; Sakamoto, Y.; Suzuki, T.; Osuna, R. M.; Casado, J.; Hernández, V. J.

- Navarrete, J. T. L.; Martinelli, N. G.; Cornil, J.; Sánchez-Carrera, R. S.; Coropceanu, V.; Brédas, J.-L. *J. Am. Chem. Soc.* **2009**, *131*, 1502–1512.
- (17) Wang, L.; Zhang, H. *J. Phys. Chem. C* **2011**, *115*, 20674–20681.
- (18) Adiga, S. P.; Shukla, D. *J. Phys. Chem. C* **2010**, *114*, 2751–2755.
- (19) Li, H.; Zheng, R.; Shi, Q. *Phys. Chem. Chem. Phys.* **2011**, *13*, 5642–5650.
- (20) Geng, Y.; Wang, J.; Wu, S.; Li, H.; Yu, F.; Yang, G.; Gao, H.; Su, Z. *J. Mater. Chem.* **2011**, *21*, 134–143.
- (21) Yin, S. W.; Li, L. L.; Yang, Y. M.; Reimers, J. R. *J. Phys. Chem. C* **2012**, *116*, 14826–14836.
- (22) Lee, C. T.; Yang, W. T.; Parr, R. G. *Phys. Rev. B* **1988**, *37*, 785–789.
- (23) Becke, A. D. *J. Chem. Phys.* **1993**, *98*, 5648–5652.
- (24) Frisch, M. J.; et al. *Gaussian 09 Revision C.01*; Gaussian Inc.: Wallingford, CT, 2009.
- (25) O'Boyle, N. M.; Tenderholt, A. L.; Langner, K. M. *J. Comput. Chem.* **2008**, *29*, 839–845.
- (26) Marcus, R. A. *Rev. Mod. Phys.* **1993**, *65*, 599.
- (27) Berlin, Y. A.; Hutchison, G. R.; Rempala, P.; Ratner, M. A.; Michl, J. *J. Phys. Chem. A* **2003**, *107*, 3970–3980.
- (28) Yin, S. W.; Yi, Y. P.; Li, Q. X.; Yu, G.; Liu, Y. G.; Shuai, Z. G. *J. Phys. Chem. A* **2006**, *110*, 7138–7143.
- (29) McMahon, D. P.; Troisi, A. *J. Phys. Chem. Lett.* **2010**, *1*, 941–946.
- (30) Brovchenko, I. V. *Chem. Phys. Lett.* **1997**, *278*, 355–359.
- (31) Norton, J. E.; Brédas, J. L. *J. Am. Chem. Soc.* **2008**, *130*, 12377–12384.
- (32) Brédas, J.-L.; Beljonne, D.; Coropceanu, V.; Cornil, J. *Chem. Rev.* **2004**, *104*, 4971–5004.
- (33) Coropceanu, V.; Cornil, J.; da Silva Filho, D. A.; Oliver, Y.; Silbey, R.; Bredas, J. L. *Chem. Rev.* **2007**, *107*, 926–952.
- (34) Reimers, J. R. *J. Chem. Phys.* **2001**, *115*, 9103–9109.
- (35) Kwon, O.; Coropceanu, V.; Gruhn, N. E.; Durivage, J. C.; Laquindanum, J. G.; Katz, H. E.; Cornil, J.; Bredas, J. L. *J. Chem. Phys.* **2004**, *120*, 8186.
- (36) Fujita, T.; Nakai, H.; Nakatsuji, H. *J. Chem. Phys.* **1996**, *104*, 2410–2417.
- (37) Troisi, A.; Orlandi, G. *J. Phys. Chem. A* **2006**, *110*, 4065–4070.
- (38) Grimme, S. *J. Comput. Chem.* **2006**, *27*, 1787–1789.
- (39) Huang, Z. W.; Sun, H.; Zhang, H. Y.; Wang, Y.; Li, F. *J. Comput. Chem.* **2011**, *32*, 2055–2063.
- (40) Chen, X.-K.; Guo, J.-F.; Zou, L.-Y.; Ren, A.-M.; Fan, J.-X. *J. Phys. Chem. C* **2011**, *115*, 21416–21428.
- (41) Yoon, M.-H.; Facchetti, A.; Stern, C. E.; Marks, T. J. *J. Am. Chem. Soc.* **2006**, *128*, 5792–5801.
- (42) Letizia, J. A.; Facchetti, A.; Stern, C. L.; Ratner, M. A.; Marks, T. J. *J. Am. Chem. Soc.* **2005**, *127*, 13476–13477.